J. Space Weather Space Clim. 4 (2014) A10
DOI: 10.1051/swsc/2014007

SWSC

RESEARCH ARTICLE OPEN ACCESS

Geomagnetically induced currents in Norway: the northernmost high-voltage power grid in the world

Minna Myllys[1,2,*], Ari Viljanen[2], Øyvind August Rui[3], and Trond Magne Ohnstad[3]

[1] Department of Physics, University of Helsinki, P.O. Box 64, 00014, Finland
[*] Corresponding author: minna.myllys@helsinki.fi
[2] Finnish Meteorological Institute, Erik Palmenin aukio 1, 00560 Helsinki, Finland
[3] Statnett, PB 4904 Nydalen, 0423 Oslo, Norway

Received 23 September 2013 / Accepted 3 February 2014

ABSTRACT

We have derived comprehensive statistics of geomagnetic activity for assessing the occurrence of geomagnetically induced currents (GIC) in the Norwegian high-voltage power grid. The statistical study is based on geomagnetic recordings in 1994–2011 from which the geoelectric field can be modelled and applied to a DC description of the power grid to estimate GIC. The largest GIC up to a few 100 A in the Norwegian grid occur most likely in its southern parts. This follows primarily from the structure of the grid favouring large GIC in the south. The magnetic field has its most rapid variations on the average in the north, but during extreme geomagnetic storms they reach comparable values in the south too. The ground conductivity has also smaller values in the south, which further increases the electric field there. Additionally to results in 1994–2011, we performed a preliminary estimation of a once per 100 year event for geoelectric field by extrapolating the statistics. We found that the largest geoelectric field value would be twice the maximum in 1994–2011. Such value was actually reached on 13–14 July 1982.

Key word. Geomagnetically Induced Currents (GIC)

1. Introduction

Space weather refers to the physical state of natural space environments. At the Earth's surface, space weather manifests itself as geomagnetically induced currents (GIC) in technological conductor networks, such as electric power transmission grids, oil and gas pipelines, telecommunication cables and railway circuits. The most famous GIC catastrophe occured in the Hydro-Quebec high-voltage system in Canada in 1989 (Bolduc 2002). It caused a blackout which lasted several hours. Other notable GIC effect was experienced in Malmö region in southern Sweden (Pulkkinen et al. 2005). Boteler et al. (1998) presented a catalogue of all published reports of geomagnetic effects on electrical systems in 1844–1996. A detailed discussion on how electric utilities are affected by GIC is presented by Molinski (2002).

Numerous GIC studies have been performed in Europe as listed by Viljanen et al. (2012). An ongoing study is the EURISGIC project (European Risk from Geomagnetically Induced Currents). In this study, we have applied the same software (Viljanen et al. 2012) and ground conductivity model (Adam et al. 2012). This work considers GIC in the Norwegian high-voltage power grid. We will first describe the methods and models, and also summarise the data sources. The main result is the statistics of GIC at the substations paying special attention to the largest events and their frequency and to the estimation of the 100-year maximum of the geoelectric field.

2. Methods and data

The recent paper by Viljanen et al. (2012) gives a comprehensive description of calculating GIC. So we only remind here that it is convenient to perform the modelling in two steps:

1. Determine the geoelectric field associated with geomagnetic variations. This is a purely geophysical problem, which is independent of the technological system.
2. Determine GIC due to the given geoelectric field in a conductor system whose topology and resistances are known.

2.1. Magnetometre data

The basic data set of the geomagnetic field comes from the continental Norwegian part of the IMAGE magnetometre network (Fig. 1), and covers years 1994–2011 with a 10-s time resolution. We have used data from 11 stations in Norway, Jäckvik (JCK) in Sweden and Kilpisjärvi (KIL) and Kevo (KEV) in Finland. Only the horizontal part of the geomagnetic field is needed to determine the geoelectric field. Table 1 shows the data coverage at the stations used. Stations with a low data availability have typically started operation in 2000s.

2.2. Ground conductivity models

We applied the ground conductivity map derived by Adam et al. (2012). It consists of rectangular blocks (Fig. 2), which have a 1-D ground model consisting of uniform layers. Concerning Norway, there are three different block models listed in Table 2. The ground conductivity of the uppermost Earth layers in the Nordic countries is generally smaller than elsewhere in Europe (Korja et al. 2002; Korja 2007). This is especially the case in South Norway.

We note that the conductivity model is not very detailed. On the other hand, the structure of the power grid defines the

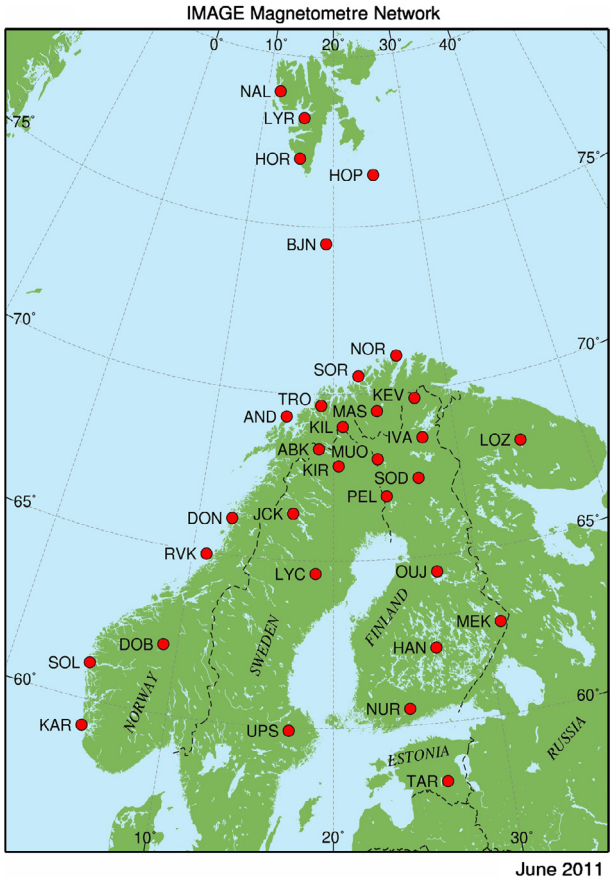

Fig. 1. IMAGE magnetometre network in northern Europe in 2011.

Table 1. Availability of data from IMAGE magnetometre stations used in this study.

Code	Full name	%
NOR	Nordkapp	19
SOR	Sørøya	89
KEV	Kevo	93
TRO	Tromsø	99
MAS	Masi	81
AND	Andenes	82
KIL	Kilpisjärvi	92
LEK	Leknes	32
JCK	Jäckvik	70
DON	Dønna	18
RVK	Rørvik	65
DOB	Dombås	66
SOL	Solund	24
KAR	Karmøya	41

relevant scale size, because GIC is basically dependent on the electric field integrated along transmission lines. In Norway, a typical distance between nodes is a few tens of kilometres (Table 3), so it is not necessary to consider features of a kilometre scale.

2.3. Power grid parameters

We considered two models of the Norwegian power grid: the present model ("2012") and a future scenario ("2030"). The latter one was considered to assess possible changes in GIC values compared to the present situation. The input to the model is

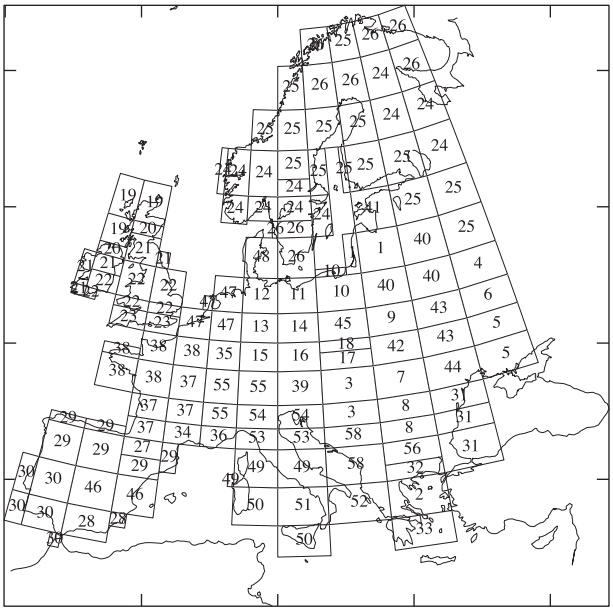

Fig. 2. Blocks of the European conductivity map Adam et al. (2012). Blocks 24–26 cover Norway (Table 2).

Table 2. Layered models of the ground conductivity applied in Norway. Layer thickness is d and resistivity ρ (= inverse of conductivity). Block numbering refers to Figure 2. Source of model parameters: http://real.mtak.hu/2957 (see also Adam et al. 2012).

Block 24		Block 25		Block 26	
d [km]	ρ [Ωm]	d [km]	ρ [Ωm]	d [km]	ρ [Ωm]
200	5000	30	5000	30	5000
Inf	200	Inf	20	Inf	200

Table 3. Characteristics of the Norwegian 2012 and 2030 high-voltage power grid models. True groundings refer to nodes with a finite earthing resistance. Average node resistance is related to true groundings and contains the transformer and earthing resistances. The average line resistance refers to all lines, also within autotransformer stations. As usual, these values correspond to the single conductor description. Lines inside stations refer to short conductor sections related to autotransformers.

	2012	2030
Nodes	162	205
True grounding	134	151
Transmission lines	174	197
Lines inside stations	27	65
Average line length [km]	40.9	42.9
Average node resistance [ohm]	0.61	0.59
Average line resistance [ohm]	0.41	0.35

the list of the substations, their locations and resistances of transformers and grounding resistances. We call the sum of the transformer and grounding resistances as earthing resistances or node resistances. The grid models contain the 400 kV and 300 kV stations and lines and one 220 kV line. There are several substations with autotransformers whose modelling followed the approach by Mäkinen (1993) and Pirjola (2005). Most stations are in the southern part of the country in both models where the grids comprise

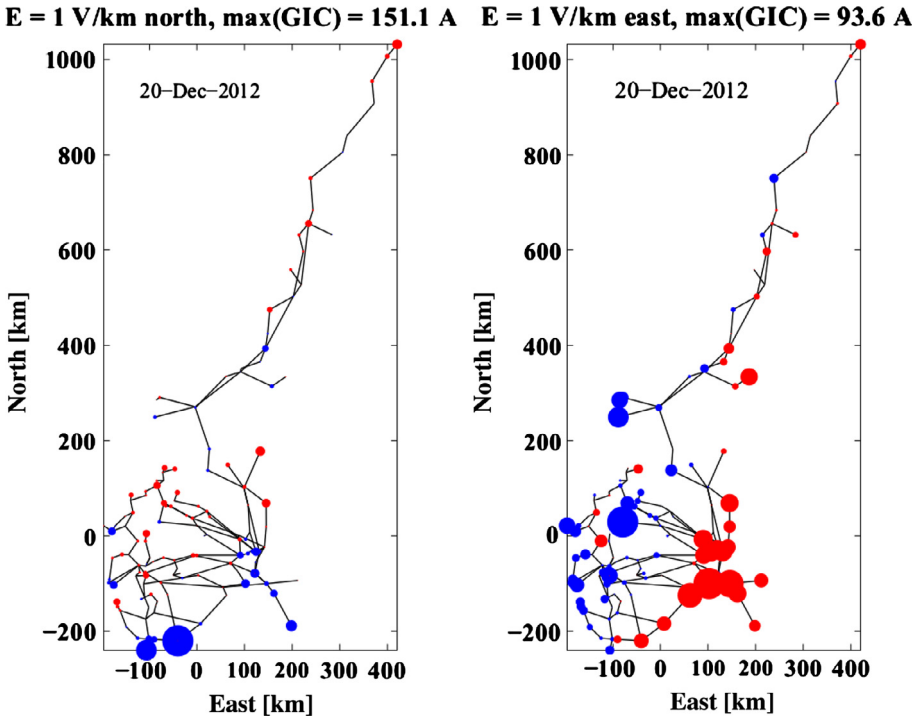

Fig. 3. GIC in the Norwegian high-voltage grid in 2012 due to a uniform electric field of 1 V km^{-1} to the north (left) or to the east (right). Blue means GIC from the ground into the grid and red is GIC from the grid into the ground.

a 2-D network. In the north, the system basically consists of one line with short branches. The main difference between the 2012 and 2030 models is that the latter has a larger number of stations and lines and a more northward extension.

There are some known inaccuracies in the grid model. The most important one is related to the grounding resistances, of which a measured value is not available at about 40 stations. In such cases, we have assumed the resistance of 0.5 Ω, which is a reasonable guess compared to typical values in Table 3. Of neighbouring countries, we have only included the nearest stations. It is important to note that nearly all substations have two or more transformers. GIC values shown in this paper are always the sum of currents through all transformers.

The simplest way to identify stations to probably experience large GIC is to assume a spatially uniform electric field. Figure 3 shows that the geometry of the grid strongly favours the occurrence of large GIC in the south. In the north, only sites close to the end point of the main transmission line can have significant GIC.

3. Results

3.1. Statistics of the time derivative of the geomagnetic field and the geoelectric field

A convenient indicator of the GIC activity level is the time derivative of the horizontal geomagnetic field ($|dH/dt|$), since it has a close relation to the geoelectric field and GIC (Viljanen 1997; Viljanen et al. 2001). We calculate the time derivative by subtracting two successive values and dividing by the 10-s time step between the values.

Generally, the time derivative becomes larger when the latitude increases. However, it is important to remark that even if the largest geomagnetic variations on average occur at high latitudes (Fig. 4), the maximum variations take place in the middle of Norway, and the difference between the maximum derivatives in the north and south becomes quite small.

Large dH/dt values can occur at any time of the year, but there is a slight preference in spring and autumn (Fig. 5). This is related to higher geomagnetic activity (Viljanen & Tanskanen 2011) around the equinox times, when Earth's magnetic dipole axis has an orientation preferring a stronger interaction between the solar wind and the geomagnetic field. At night-time, geomagnetic variations are the largest (Fig. 5) which is due to the enhanced ionospheric current systems related to the auroral activity. Figure 5 shows the daily maximum of dH/dt at Tromsø in 1994–2011. Comparably large values of time derivatives occur almost every year even if there is a generally decreased geomagnetic activity like in 2009–2011.

GIC is directly related to the geoelectric field which depends on the ground conductivity: the smaller the conductivity the larger the electric field, assuming a geomagnetic field variation of a fixed amplitude. The latitude dependence of the average geoelectric field is affected by two factors: the northward increase of dH/dt and spatial variability of the ground conductivity. When studying only the yearly maximum field, the situation changes quite drastically. The maximum dH/dt values are quite comparable at all locations in Norway, as shown in Figure 4. Due to the small conductivities in the south, it finally appears that the maximum electric fields occur in the southern part of the country as shown in Figure 6

The seasonal variation of the daily maximum electric field shows a preference of large values in spring and autumn similarly to dH/dt. Daily variation of the hourly maximum has a maximum around the local midnight similarly to dH/dt.

3.2. Statistics of GIC

As expected by the results in previous sections, due to the geometry of the grid and small ground conductivities giving

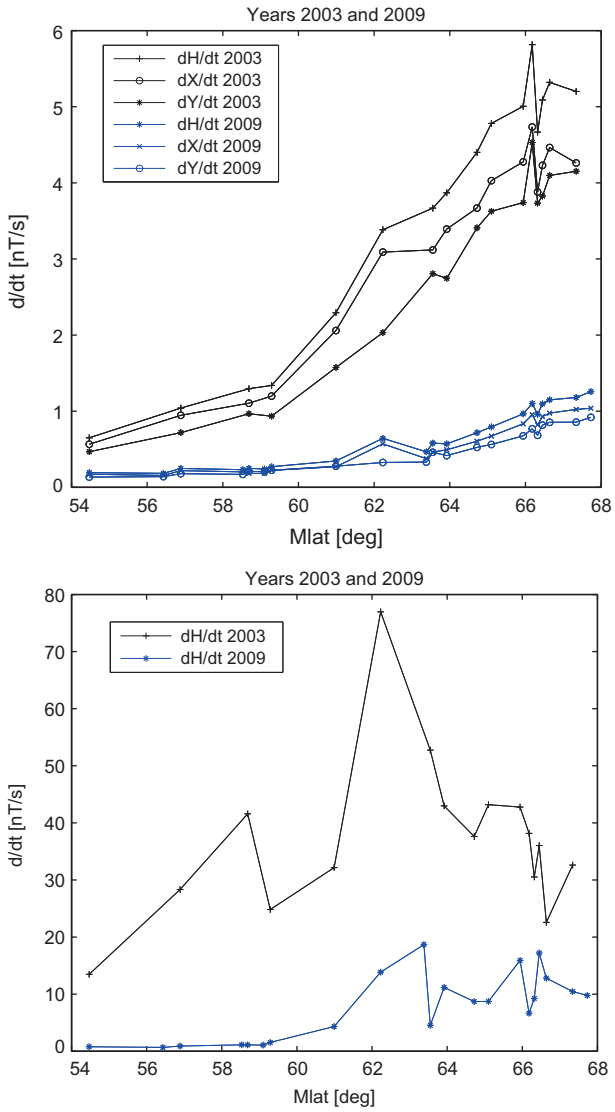

Fig. 4. Average daily maximum of the time derivative of the 10-s geomagnetic field and maximum of the time derivative of the horizontal geomagnetic field as a function of geomagnetic latitude in 2003 and 2009. Year 2003 represents a very active time and 2009 is geomagnetically quiet.

rise to large electric fields in the south, the largest GIC occur in southern Norway (Fig. 7). The largest modelled 10-s values in the Norwegian 300 kV and 400 kV grids are about 400 A. However, GIC values exceeding 100 A are still very rare. Such values are not reached at all stations and they do not occur every year.

We repeated the same calculations for the 2030 grid model. The largest GIC will still occur in South Norway and reach values up to about 400 A as in the 2012 model. The only more significant exception is that the northernmost station in the end of a new 400 kV line have had GIC up to about 200 A. In the present grid, there is not such a local prominent maximum in the north as is also evident from Figure 3.

As a case example, we discuss briefly the storm on 29 October 2003. A special feature is the global sudden impulse in the magnetic field due to a strong solar wind pulse at the beginning of the storm at about 06:11 UT. The magnetometre station at Rørvik in the west coast recorded $|dH/dt|$ as high as 77 nT s^{-1}, which is the largest value ever reported in the Nordic countries (Pulkkinen et al. 2005). Followed by this, the rest of day was highly active according to the sum of GIC at all nodes of the power grid (Fig. 8). Figure 9 shows snapshots of the interpolated dH/dt and the electric field during the most intense phases of the event on 06:11:40–06:12:10. There is a zone of extremely large dH/dt values at 06:11:40 from West Norway to North Finland. The spatial structure of the fields has a rapid variation between the time steps and also a strong variability between different regions.

3.3. Extremes of GIC

The statistics presented in the previous section is based on a 18-year period, which corresponds to about 1.5 sunspot cycles. It is still relatively quite a short time, and it does not contain the largest known geomagnetic storms. Consequently, we extended the results to find out a "once per 100-year case".

Following the approach by Pulkkinen et al. (2008, 2012), we have estimated the distribution of the electric field values in a 100-year period. We have fitted two curves to the electric field values to extrapolate the largest magnitude of the 10-s value occurring once in 100 years. The fitted curves have the exponential forms

$$y = ae^{bx^2+cx+d}, \quad (1)$$

for the blue curve in Figure 10, and

$$y = ae^{bx+c}, \quad (2)$$

for the green curve. Here x is the logarithm of the value of the electric field and a, b, c, d are constant. We have only used data points in the tail of the distribution. The small electric field values are more common than the large one, but the largest electric field values are related to fast and large changes in magnetic field during ionospheric substorms. Thus, it is relevant to use only large electric field values for the extrapolation. In terms of GIC, the small electric field values are not interesting. In both fitted curves, the number of data points that have been used varies. A larger number of data points (101) were used for fitting the blue curve than the green curve (81). The total number of data points was 200. We used two different fitted curves, because it was impossible to find a single method which fits to the data points of all stations. Table 4 summarises the results and compares them to the modelled maximum in 1994–2011. As a rule of thumb, the once in 100 years field can be about 1.5–2 times larger than that modelled for the period of 1994–2011.

We performed a case study of the large storm in 13–14 July 1982. This is probably the largest magnetic storm at some parts of the Nordic countries at least since 1982 as measured by the maximum dB/dt. For example, at Nurmijärvi in south Finland the maximum time derivative was about 40 nT s^{-1} (from 10-s values) (Viljanen 1997). Its notable magnitude was also pointed out by Kappenman (2005). This storm also caused problems in Swedish power grid (Wallerius 1982; Wik et al. 2009). We recalculated results for 1994–2011 from 1-min average of the geomagnetic field, because 1-min is the best temporal resolution available for 1982. We also used a single ground conductivity model (block 24, Table 2) because it gives the most reasonable way to compare events when using data from sites outside of Norway. The largest modelled 1-min electric field values in southern part of Norway in 1994–2011 are around 3.4–2.2 V km^{-1} and the largest extrapolated 100 year maximums are around 4.55–2.15 V km^{-1}.

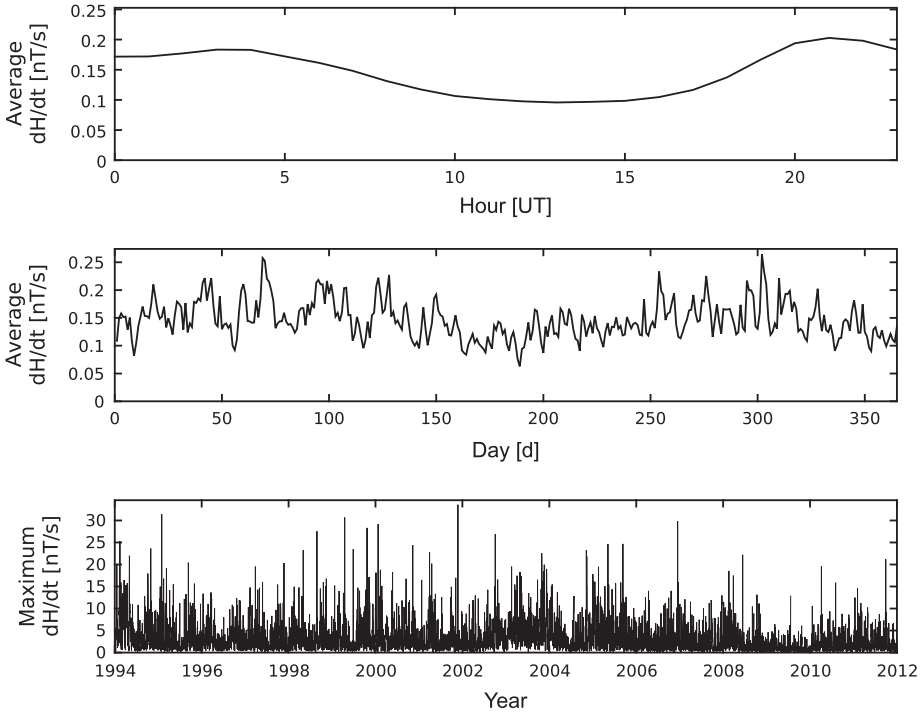

Fig. 5. Average value of the hourly maximum of the time derivative of the geomagnetic field, average value of the daily maximum of the time derivative of the geomagnetic field and daily maximum of the time derivative of the geomagnetic field at Tromsø in 1994–2011.

The 13–14 July 1982 geomagnetic field data come from the observatory at Sodankylä and Nurmijärvi, Swedish observatory at Lovö, the Danish observatory Brorfelde and the German observatory Wingst. Table 5 shows maximum time derivatives of the horizontal magnetic field and maximum electric fields on 13–14 July 1982. The ground conductivity model of block 24 has been used when electric field values were computed. The largest electric field value (8.04 V km^{-1}) on 13–14 July 1982 occurred in Nurmijärvi and the smallest (2.52 V km^{-1}) in Wingst.

The July 1982 storm was about twice as large when defined by the maximum electric field in 1994–2011. It has also approximately equal or even slightly larger magnitudes as the estimated once per 100 year event. Because the extrapolation method is quite simple, some care is needed when interpreting the results. However, it is clear that the July 1982 strom was definitely much larger than any event observed in 1994–2011.

3.4. Validity of results

Due to the lack of long-term proper DC recordings at Norwegian substations, we cannot directly compare the modelled and measured GIC. However, the modelled GIC values can be compared to GIC recordings from nearby countries to discuss the validation of the used models. In Finland in the end of 1970s, Fingrid recorded GIC at a four transformer stations. At this time, there were not yet neutral-point reactors with large DC resistances, so the grounding resistances at substations were quite equal to the present Norwegian grid. The largest 10-s value at Huutokoski was 165 A on 4 January 1979 (Pirjola 1983). The largest GIC ever in Finland was measured on 24 March 1991 at Rauma reaching 200 A as a 1-min value (Elovaara et al. 1992), so the 10-s maximum must have been even larger. In 1996–2008, Fingrid performed measurements at three transformer neutrals in Finland (Pirttikoski, Rauma, Ylikkälä). The largest value in 1996–2008 was about 40 A at Pirttikoski (30 October 2003), 42 A at Rauma (30 October 2003) and 27 A at Yllikkälä (15 July 2000). The resistances at the transformer stations were then 1–3 Ω. If they were about 0.5 Ω as in Norway then we can roughly estimate that 100 A would have reached at these Finnish sites.

The largest GIC values at a substation in southern Sweden are 269 A on 6 April 2000, 222 A on 15 July 2000 (Wik et al. 2008) and 200 A on 30 October 2003 (Wik et al. 2009). Southern Sweden has similar ground structures as Norway. These Swedish maximum values are close to the largest modelled GIC in Norway. Making the apparently reasonable assumption that the Swedish power grid is quite similar to the Norwegian one, this gives support to the estimations made in this study.

4. Conclusions

There are three factors contributing to the occurrence of GIC: geometry of the grid, spatial variations of the geomagnetic field, and spatial variations of the ground conductivity. The largest GIC in the Norwegian grid occur most likely in its southern parts. This follows primarily from the structure of the grid favouring large GIC in the south. The magnetic field has its most rapid variations (time derivative dB/dt) on the average in the north, but during extreme geomagnetic storms dB/dt reaches comparable values in the south too. Finally, the ground conductivity has smaller values in the south, which further increases the electric field there.

Statistical results are based on 10-s geomagnetic data in 1994–2011 and block models of the ground conductivity. The largest modelled 10-s GIC values in the Norwegian 300 kV and 400 kV grids are about 400 A (in the neutral lead), and there are 15 substations where GIC can reach about 200 A.

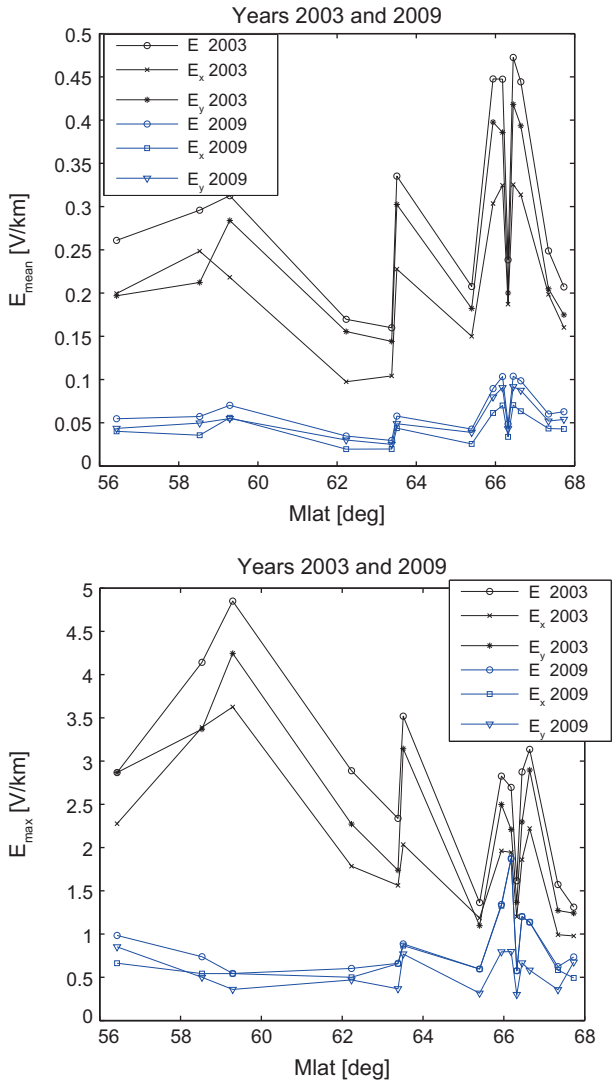

Fig. 6. Average daily maximum and maximum of the modelled 10-s electric field as a function of geomagnetic latitude in 2003 and 2009. Year 2003 represents a very active time and 2009 is geomagnetically quiet.

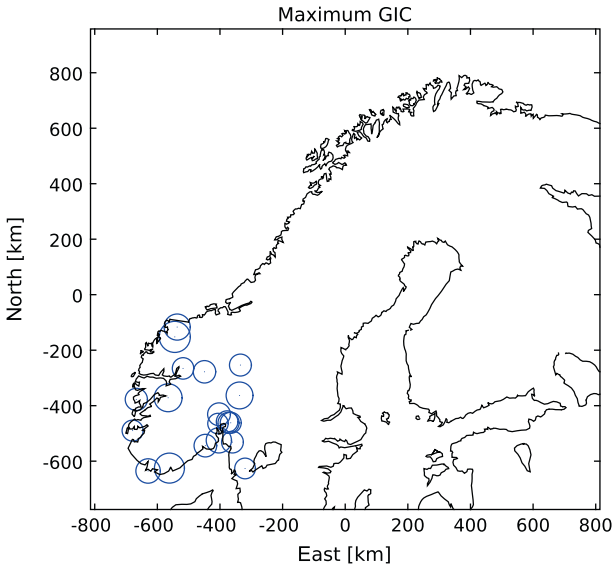

Fig. 7. Stations with the largest GIC in 1994–2011. The size of the circle is proportional to the amplitude of GIC. The maximum is about 400 A.

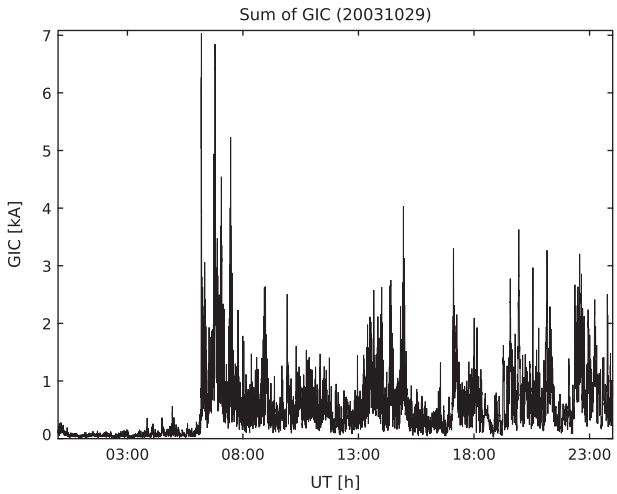

Fig. 8. Sum of GIC in the nodes of the Statnett 2012 grid assuming the event on 29 October 2003.

On the other hand, the number of 10-s GIC values exceeding 100 A is typically only 10–50 in 1994–2011, and such values do not occur at all stations.

We estimated an extreme event occurring once in 100 years by extrapolating the statistics. During such a case, the electric field and GIC can be about 1.5–2 times larger than that modelled for the period of 1994–2011. Such an event has probably happened on 13–14 July 1982.

We also considered the model of the expected future grid in 2030. The main results obtained for the present grid are valid also for the future one. The largest GIC will still occur in South Norway and have nearly equal amplitudes up to 400 A at maximum as in 2012. The only major exception is that the northernmost station in the end of the new 400 kV line will likely experience GIC of about 200 A.

Based on the identified uncertainties in the ground conductivity models and power grid models, we can give the following general guidelines in interpreting the results: (1) The models give a good indicator of stations with potentially large GIC (2) The largest GIC events in 1994–2011 are identified reliably (3) Based on GIC data from neighbouring countries, we can consider the order of magnitudes of Norwegian estimations to be correct (4) Despite some uncertainty in the modelled GIC amplitudes, statistical results are reliable when applied in a relative sense. In other words, it is advisable to scale the results with respect to the maximum case.

As a suggestion for further studies to improve the validation of especially the ground conductivity models, we recommend continuous GIC recordings as direct DC measurements at selected stations. That should preferably happen close to a magnetometre station and at a station where the geometry of the grid favours large GIC. Such measurements would help to check the grid model and to fix the ground conductivity model.

Acknowledgements. We thank the University of Tromsø for providing an extensive high-quality time series of geomagnetic recordings for this study. Some older recordings before the study period were obtained from the World Data Centre for Geomagnetism (Edinburgh). This work exploited the software developed by the Finnish Meteorological Institute within the EURISGIC project (European Risk from Geomagnetically Induced Currents) funded

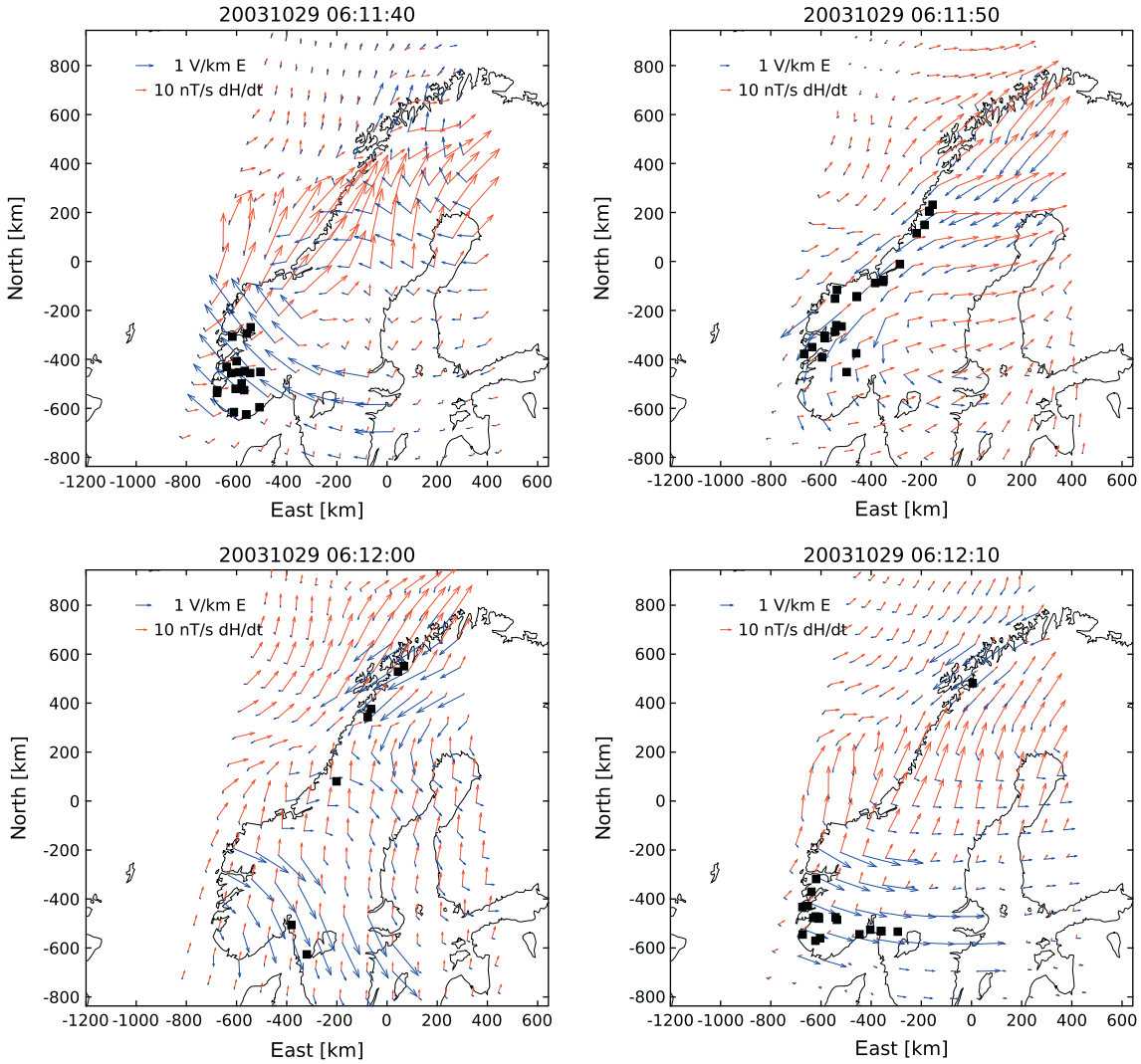

Fig. 9. Beginning of the magnetic storm on 29 October 2003 at 06:11:40–06:12:10 UT. Red arrows: time derivative of the horizontal magnetic field, blue arrows: electric field. Black small dots indicate the transformers stations at which the daily maximum GIC occurred at the given time step.

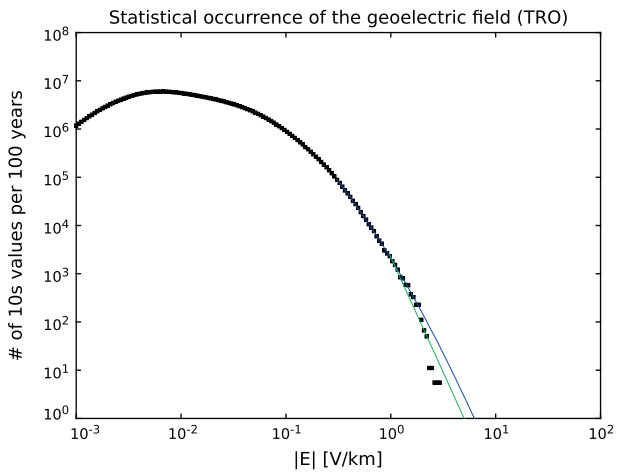

Fig. 10. Statistical occurrence of 10-s electric field values per 100 years at Tromsø. Coloured lines correspond to two different extrapolation methods explained in the text.

Table 4. The largest modelled 10-s value of the horizontal electric field (E_{max}) in 1994–2011 at selected IMAGE magnetometre stations, and the extrapolated maximum value occurring once in 100 years, as obtained by two different methods. The full conductivity model has been used.

Station	E_{max} [V/km]	Blue	Green
AND	3.0	5.1	4.9
DON	2.3	3.0	1.8
JCK	3.5	5.1	4.6
KAR	3.3	5.9	6.4
KEV	3.1	3.9	4.3
KIL	2.8	5.0	4.8
LEK	1.4	3.0	1.7
MAS	1.8	2.1	1.6
NOR	1.3	2.6	1.4
RVK	2.9	4.7	5.4
SOL	4.1	6.7	7.6
SOR	1.6	2.2	1.8
TRO	3.0	6.3	5.0

Table 5. Maximum time derivative of the 1-min horizontal magnetic field and maximum horizontal electric field on 13–14 July 1982 at a few observatories listed from the north to south. The ground conductivity model of block 24 in Table 2 has been used.

Observatory	$\lvert dH/dt\rvert$ [nT s^{-1}]	$\lvert E_{hor}\rvert$ [V km^{-1}]
Sodankylä (FI)	33.3	7.78
Nurmijärvi (FI)	19.9	8.04
Lovö (SE)	44.8	8.67
Brorfelde (DK)	24.5	6.79
Wingst (DE)	8.0	2.52

from the European Community's Seventh Framework Programme (FP7/2007-2013) under Grant Agreement No. 260330.

References

Adam, A., E. Pracser, and V. Wesztergom, Estimation of the electric resistivity distribution (EURHOM) in the European lithosphere in the frame of the EURISGIC WP2 project, *Acta Geod. Geophys. Hung.*, **47**, 377–387, DOI: 10.1556/AGeod.47.2012.4.1, 2012.

Bolduc, L., GIC observations and studies in the Hydro-Quebec power system, *J. Atmos. Sol. Terr. Phys.*, **64 (16)**, 1793–1802, 2002.

Boteler, D.H., R.J. Pirjola, and H. Nevanlinna, The effects of geomagnetic disturbances on electrical systems at the earth's surface, *Adv. Space Res.*, **22**, 17–27, DOI: 10.1016/S0273-1177(97)01096-X, 1998.

Elovaara, J., P. Lindblad, A. Viljanen, T. Mäkinen, R. Pirjola, S. Larsson, and B. Kielén, Geomagnetically induced currents in the Nordic power system and their effects on equipment, control, protection and operation, Paper 36-301 of the Proceedings of the CIGRE 1992 Session, 30 August–5 September, Paris, 10 pp., 1992.

Kappenman, J.G., An overview of the impulsive geomagnetic field disturbances and power grid impacts associated with the violent Sun-Earth connection events of 29–31 October 2003 and a comparative evaluation with other contemporary storms, *Space Weather*, **3**, S08C01, DOI: 10.1029/2004SW000128, 2005.

Korja, T., How is the European Lithosphere Imaged by Magnetotellurics? *Surv. Geophys.*, **28**, 239–272, DOI: 10.1007/s10712-007-9024-9, 2007.

Korja, T., M. Engels, A.A. Zhamaletdinov, A.A. Kovtun, N.A. Palshin, M.Yu. Smirnov, A.D. Tokarev, V.E. Asming, L.L. Vanyan, I.L. Vardaniants, and BEAR Working Group, Crustal conductivity in Fennoscandia a compilation of a database on crustal conductance in the Fennoscandian Shield, *Earth Planets Space*, **54**, 535–558, 2002.

Mäkinen, T., *Geomagnetically induced currents in the Finnish power transmission system*, **32**, Finnish Meteorological Institute Geophysical Publications, 101 p., 1993.

Molinski, T.S., Why utilities respect geomagnetically induced currents, *J. Atmos. Sol. Terr. Phys.*, **64**, 1765–1778, 2002.

Pirjola, R., Induction in power transmission lines during geomagnetic disturbances, *Space Sci. Rev.*, **35**, 185–193, 1983.

Pirjola, R., Effects of space weather on high-latitude ground systems, *Adv. Space Res.*, **36**, 2231–2240, DOI: 10.1016/j.asr.2003.04.074, 2005.

Pulkkinen, A., S. Lindahl, A. Viljanen, and R. Pirjola, October 29–31, 2003 geomagnetic storm: geomagnetically induced currents and their relation to problems in the Swedish high-voltage power transmission system, *Space Weather*, **3**, S08C03, DOI: 10.1029/2004SW000123, 2005.

Pulkkinen, A., R. Pirjola, and A. Viljanen, Statistics of extreme geomagnetically induced current events, *Space Weather*, **6**, S07001, DOI: 10.1029/2008SW000388, 2008.

Pulkkinen, A., E. Bernabeu, J. Eichner, C. Beggan, and A.W.P. Thomson, Generation of 100-year geomagnetically induced current scenarios, *Space Weather*, **10**, S04003, DOI: 10.1029/2011SW000750, 2012.

Viljanen, A., The relation between geomagnetic variations and their time derivatives and implications for estimation of induction risks, *Geophys. Res. Lett.*, **24**, 631–634, 1997.

Viljanen, A., and E. Tanskanen, Climatology of rapid geomagnetic variations at high latitudes over two solar cycles, *Ann. Geophys.*, **29**, 10, 2011.

Viljanen, A., H. Nevanlinna, K. Pajunpää, and A. Pulkkinen, Time derivative of the horizontal geomagnetic field as an activity indicator, *Ann. Geophys.*, **19**, 1107–1118, http://www.ann-geophys.net/19/1107/2001/angeo-19-1107-2001.pdf, 2001.

Viljanen, A., R. Pirjola, M. Wik, A. Adam, E. Pracser, Ya. Sakharov, and J. Katkalov, Continental scale modelling of geomagnetically induced currents, *J. Space Weather Space Clim.*, **2**, A17, http://dx.doi.org/10.1051/swsc/2012017, 2012.

Wallerius, A., Solen gav Sverige en strömstöt, *Ny teknik*, teknisk tidskrift, **29**, 3, 1982.

Wik, M., A. Viljanen, R. Pirjola, A. Pulkkinen, P. Wintoft, and H. Lundstedt, Calculation of geomagnetically induced currents in the 400 kV power grid in Southern Sweden, *Space Weather*, **6**, S07005, DOI: 10.1029/2007SW000343, 2008.

Wik, M., R. Pirjola, H. Lundstedt, A. Viljanen, P. Wintoft, and A. Pulkkinen, Space weather events in July 1982 and October 2003 and the effects of geomagnetically induced currents on Swedish technical systems, *Ann. Geophys.*, **27**, 1775–1787, 2009.

Cite this article as: Myllys M, Viljanen A, Rui ØA & Ohnstad TM: Geomagnetically induced currents in Norway: the northernmost high-voltage power grid in the world. J. Space Weather Space Clim., 2014, **4**, A10.